AGU PUBLICATIONS

Geophysical Research Letters

RESEARCH LETTER
10.1002/2014GL059383

Key Points:
- Magnetospheric relativistic electron fluxes are enhanced during HILDCAAs
- Enhancements of relativistic electron fluxes vary with solar cycle phases
- Enhancements are higher in declining/minimum phases than rising/maximum phases

Correspondence to:
R. Hajra,
rajkumarhajra@yahoo.co.in

Citation:
Hajra, R., B. T. Tsurutani, E. Echer, and W. D. Gonzalez (2014), Relativistic electron acceleration during high-intensity, long-duration, continuous *AE* activity (HILDCAA) events: Solar cycle phase dependences, *Geophys. Res. Lett.*, *41*, 1876–1881, doi:10.1002/2014GL059383.

Received 22 JAN 2014
Accepted 11 MAR 2014
Accepted article online 20 MAR 2014
Published online 31 MAR 2014

Relativistic electron acceleration during high-intensity, long-duration, continuous *AE* activity (HILDCAA) events: Solar cycle phase dependences

Rajkumar Hajra[1], Bruce T. Tsurutani[2], Ezequiel Echer[1], and Walter D. Gonzalez[1]

[1]Instituto Nacional de Pesquisas Espaciais (INPE), São José dos Campos, São Paulo, Brazil, [2]Jet Propulsion Laboratory, California Institute of Technology, Pasadena, California, USA

Abstract High-intensity, long-duration, continuous *AE* activity (HILDCAA) intervals during solar cycle 23 (1995–2008) have been studied by a superposed epoch analysis. It was found that HILDCAA intervals order the solar wind velocity, temperature and density (characteristic of high-speed solar wind intervals), the polar cap potential, and various other geomagnetic indices well. The interplanetary magnetic field B_z is generally negative, and the Newell solar wind coupling function is high during HILDCAA events. The HILDCAA intervals are well correlated with an enhancement of magnetospheric relativistic ($E > 2$ MeV) electron fluxes observed at geosynchronous orbit with a delay of ~1.5 days from the onset of the HILDCAAs. The response of the energetic electrons to HILDCAAs is found to vary with solar cycle phase. The initial electron fluxes are lower for events occurring during the ascending and solar maximum (AMAX) phases than for events occurring during the descending and solar minimum (DMIN) phases. The flux increases for the DMIN phase events are >50% larger than for the AMAX phase events. Although the solar wind speeds during the DMIN phases were slightly higher and lasted longer than during the AMAX phases, no other significant solar wind differences were noted. It is concluded that electrons are accelerated to relativistic energies most often and most efficiently during the DMIN phases of the solar cycle. We propose two possible solar UV mechanisms to explain this solar cycle effect.

1. Introduction

It has been speculated by *Tsurutani et al.* [2010] and *Hajra et al.* [2013] that enhanced magnetospheric relativistic electrons are associated not only with solar wind high-speed streams (HSSs) [*Paulikas and Blake*, 1979] but more directly with high-intensity, long-duration, continuous *AE* activity (HILDCAA) events at the Earth [*Tsurutani and Gonzalez*, 1987]. A simplified version of the hypothesis is as follows: Alfvén waves are generated by supergranule circulation at the Sun [*Alfvén*, 1942]. The waves are convected to 1 *AU* and beyond by the solar wind [*Belcher and Davis*, 1971; *Tsurutani et al.*, 1994]. The southward components of the Alfvén waves cause magnetic reconnection at the Earth's dayside magnetopause, leading to substorm/convection events and energetic (10–100 keV) electron injection into the nightside sector of the magnetosphere [*DeForest and McIlwain*, 1971; *Tsurutani and Gonzalez*, 1987; *Horne and Thorne*, 1998]. The temperature anisotropy of the heated electrons leads to plasma instability, generating electromagnetic plasma waves called chorus [*Kennel and Petschek*, 1966; *Tsurutani and Smith*, 1974, 1977]. Resonant interactions of the chorus waves with the electrons lead to the acceleration of electrons to relativistic energies [*Inan et al.*, 1978; *Horne and Thorne*, 1998, 2003; *Summers et al.*, 1998, 2007; *Horne et al.*, 2003a, 2003b; *Thorne et al.*, 2005; *Tsurutani et al.*, 2009, 2013].

The aim of this effort is to determine if relativistic electron enhancements occur during HILDCAA intervals, and if so, more can be learned about the production and loss processes. A superposed epoch analysis is applied to deduce the general characteristics of the solar wind/interplanetary parameters, geomagnetic variations, and magnetospheric relativistic electrons during HILDCAA intervals. We will study the entire solar cycle (SC) 23 from 1995 through 2008. This will allow investigation of the solar cycle phase dependence of relativistic electron acceleration, if there is any. This is the first study of relativistic electron production during HILDCAA intervals.

2. Data Analyses and Results

HILDCAAs are, by definition, intense auroral activity intervals characterized by peak *AE* intensities greater than 1000 nT, a minimum of 2 days duration, where *AE* values do not drop below 200 nT for more than 2 h at a

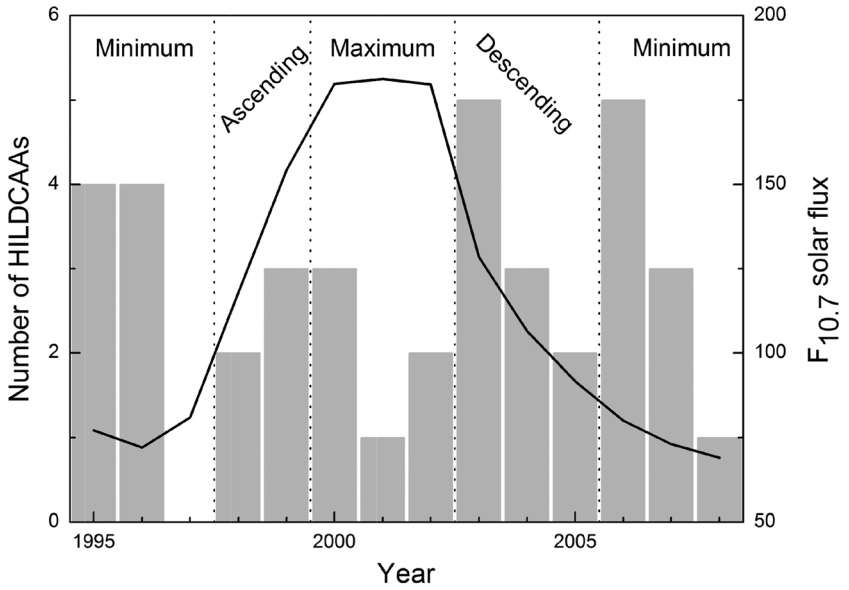

Figure 1. Histograms show the number of HILDCAA events during each year of observations (left *y* axis). The solid line shows the annual averaged $F_{10.7}$ solar flux (10^{-22} W m^{-2} Hz^{-1}) (right *y* axis). The phases of the solar cycle are separated by vertical dotted lines and mentioned in the figure.

time [*Tsurutani and Gonzalez*, 1987]. These events are also defined to occur outside the main phases of geomagnetic storms. These strictly defined "HILDCAA criteria" are used to separate them from mechanisms that create magnetic storm main phases. For a more detailed discussion on this topic and the process of event selection, interested readers are referred to *Tsurutani et al.* [2004, 2011], *Guarnieri* [2006], and *Hajra et al.* [2013, 2014]. From a list of HILDCAA events during ~3.5 solar cycles (1975–2011) prepared by *Hajra et al.* [2013], we selected the 38 events that occurred during the most recent solar cycle (SC 23) when solar wind/interplanetary and relativistic electron data are almost continuously available [*Hajra et al.*, 2014].

For the superposed epoch analyses, we have used the solar wind/interplanetary and geomagnetic data from the OMNI2 database and the integrated fluxes (in the unit of cm^{-2} s^{-1} sr^{-1}) of electrons with energy >2 MeV from the Geostationary Operational Environmental Satellites (GOES) 8, 11, and 12. The satellites carry space environment monitor instrument subsystems onboard that provide magnetometer, energetic particle, and soft X-ray data. The electron fluxes used in the present study were measured by solid-state detectors with pulse height discrimination in the energetic particle sensor. The data were corrected for secondary responses from other energies (e.g., protons >32 MeV) and from directions outside the nominal detector entrance aperture.

We separated the events according to their occurrence in different solar cycle phases, namely, the ascending phase (1998–1999), solar maximum (2000–2002), the descending phase (2003–2005), and the solar minimum phase (1995–1997 and 2006–2008). Figure 1 shows the distribution of the events of this study divided into different solar cycle phases. For our statistical studies, we combine the events occurring during the ascending and solar maximum and call them the AMAX events. We also combine the events occurring during the descending phase and solar minimum and call them the DMIN events. The present study involves 11 AMAX events and 27 DMIN events. We formed these two groupings for two reasons: First, it was shown by *Hajra et al.* [2013] that the properties of HILDCAAs, like *AE* intensity and duration, are comparable during the descending phase and solar minimum and likewise during the ascending phase and solar maximum. DMIN phase events are >20% longer in duration than the AMAX phase events. The second reason is that there is a lack of sufficient number of events to conduct statistical study if we consider the phases separately (see Figure 1).

2.1. Solar Wind Dependences

Figure 2 shows the superposed solar wind parameter profiles for all of the HILDCAA intervals. The reference time ($t = 0$) is the time of HILDCAA initiation (based on the criteria stated previously). From top to bottom, the

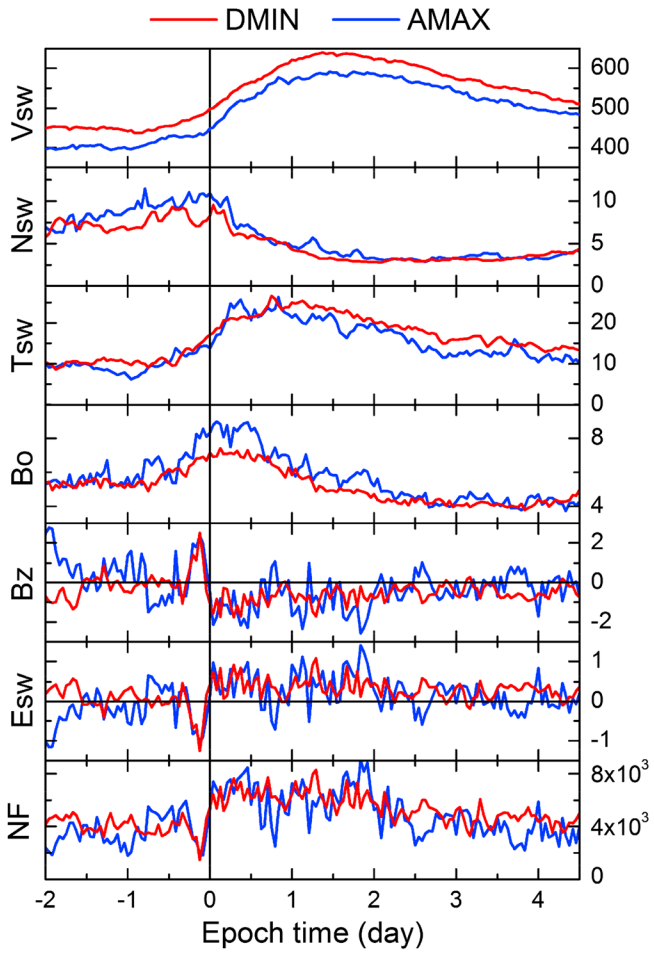

Figure 2. Superposed time series of solar wind parameters for HILDCAA events. (top to bottom) The solar wind speed (V_{sw} in km/s), the density (N_{sw} in cm^{-3}), the proton temperature (T_{sw} in 10^4 K), the IMF strength (B_o in nT), the north-southward component of the IMF (B_z in nT), the interplanetary dawn-to-dusk electric field (E_{sw} in mV/m), and the solar wind driver given by Newell function. The zero epoch time (indicated by vertical line) corresponds to the initiation of HILDCAAs. The red and blue lines stand for HILDCAA events occurring during DMIN phases and AMAX phases, respectively.

panels are the solar wind speed (V_{sw}), density (N_{sw}), temperature (T_{sw}), the interplanetary magnetic field magnitude (IMF B_o) and B_z component (in GSM coordinates), the solar wind dawn-to-dusk electric field (E_{sw}), and the solar wind "driver function" given by the Newell function (NF) parameter: $V_{sw}^{4/3} B_T^{2/3} \sin^{8/3}(\theta/2)$, where B_T is the IMF perpendicular to the Sun-Earth line and θ is the IMF clock angle [*Newell et al.*, 2007]. The DMIN events are shown in red, and the AMAX events are shown in blue. E_{sw} is a proxy for the coupling between the solar wind and the magnetosphere. According to *Newell et al.* [2007], the NF parameter has been shown to correlate with the geomagnetic indices better than other solar wind-magnetosphere coupling functions.

The variations of solar wind/interplanetary data show typical signatures of corotating interaction regions (CIRs) [*Smith and Wolfe*, 1976; *Tsurutani et al.*, 1995], i.e., compressions in plasma and magnetic fields at the interface between the HSS and slow stream in the antisolar direction (upstream) of the HSS. One can note several interesting features in this figure. The HILDCAA interval starts at the positive gradients of high-speed streams (Figure 2, first panel) and temperatures (Figure 2, third panel). The magnetic field magnitude still crests slightly to the right of $t = 0$, because some CIRs which did not cause magnetic storms are included in this plot (a superposition of many HILDCAA events). The $t = 0$ time clearly defines the sharp southward turning of the IMF B_z and the enhancements of the interplanetary electric field E_{sw} and the NF coupling term. It is quite remarkable how well the superposed HILDCAA events order the various different interplanetary parameters.

Figure 2 shows that the solar wind/interplanetary variations exhibited more or less similar trends during both solar cycle phase intervals. IMF B_o and T_{sw} show some systematic differences between the DMIN and AMAX phases, although the differences were less than the 1σ levels. However, some significant differences can be noted in the solar wind velocity panel (Figure 2, first panel). The peak HSS speed was higher for the DMIN events (~650 km/s) than the AMAX events (~590 km/s). The HSSs also persisted for longer time in DMIN phases than in AMAX phases on average (not shown).

2.2. Geomagnetic and Radiation Belt Effects

Figure 3 shows the variations of the polar cap index (PCI) and the geomagnetic indices: *Kp*, *Dst*, *AL*, and *AE* along with the fluxes of magnetospheric relativistic (>2 MeV) electrons for the HILDCAAs occurring during the DMIN (red) and AMAX (blue) phases. The PCI values are closely related with the dayside reconnection rate

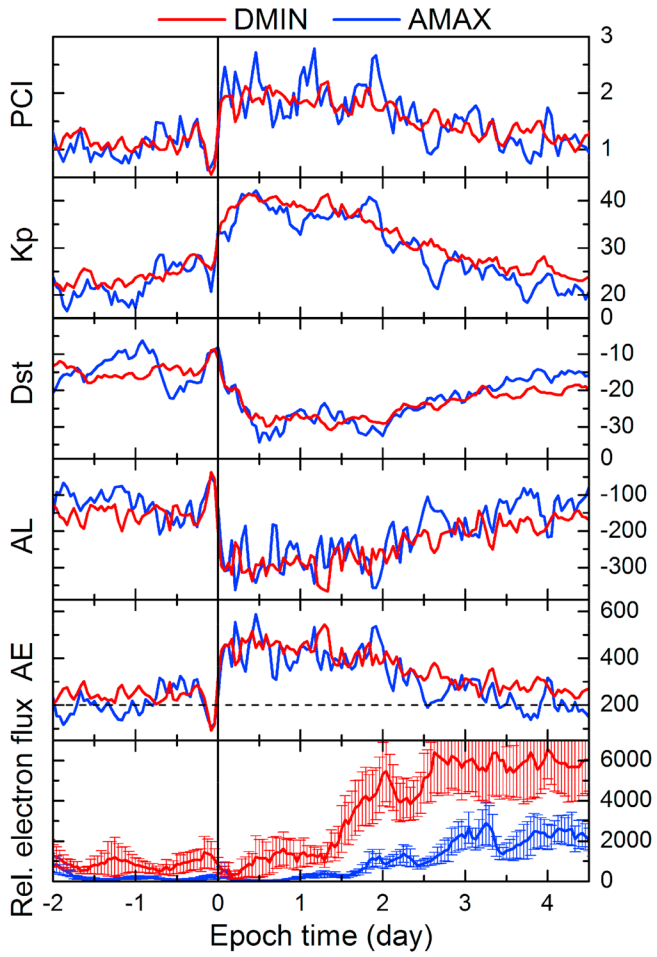

Figure 3. Superposed time series of the polar cap index, *Kp*, *Dst* (nT), *AL* (nT) and *AE* (nT) indices, and relativistic electron fluxes ($cm^{-2}\,s^{-1}\,sr^{-1}$) from GOES during HILDCAAs. The red and blue lines correspond to DMIN and AMAX phases, as before. The horizontal dashed line in the *AE* panel indicates the *AE* = 200 nT level. (bottom) Vertical bars indicate the standard deviations of the mean fluxes.

by IMF B_z southward components. *Kp* is a midlatitude geomagnetic index and a proxy for global magnetospheric convection, *Dst* gives a quantitative measure of the ring current or partial ring current, and the *AL* and *AE* indices indicate auroral region substorm activity. All of the above parameters are likewise well ordered by the HILDCAA intervals. We found no obvious/significant differences in the geomagnetic index variations during the DMIN and AMAX phase events.

The most interesting results of the analyses are shown in Figure 3 (bottom), the relativistic electron flux variations. For the DMIN events, the fluxes decreased from their average initial flux levels of $>1000\,cm^{-2}\,s^{-1}\,sr^{-1}$ to the lowest values ("flux dropout" $\sim 254\,cm^{-2}\,s^{-1}\,sr^{-1}$), ~4 h after the HILDCAA event initiation. The fluxes recovered to the preevent values within ~10 h of the dropout. For the AMAX events, the fluxes decreased from the average initial levels of $\sim 800\,cm^{-2}\,s^{-1}\,sr^{-1}$ to their lowest values ($\sim 32\,cm^{-2}\,s^{-1}\,sr^{-1}$) at t~15 h. They took longer (>1 day) to recover to the preevent flux values than for the DMIN events.

The relativistic electron fluxes for both grouped solar cycle phases (DMIN and AMAX) start to increase at approximately 1.5 days after the onset of the HILDCAA event ($t = 0$). A maximum flux of $\sim 6379\,cm^{-2}\,s^{-1}\,sr^{-1}$ was recorded during the DMIN events. It is ~5 times the value of preevent fluxes. The maximum enhanced flux value for the AMAX events was $\sim 2884\,cm^{-2}\,s^{-1}\,sr^{-1}$, ~3.5 times the corresponding preevent values. The AMAX event peak flux was less than 50% of the value of peak fluxes for the DMIN events. To test if the differences in the superposed fluxes in two groupings are statistically significant, we calculated the standard (1σ) deviations of the mean fluxes (shown in the figure by vertical bars). During the HILDCAA intervals, the mean fluxes in the DMIN and AMAX phases are outside of the 1σ levels of one another. This can be interpreted to mean that there are statistically different values in the two phases. The other solar wind and geomagnetic parameters in Figures 1 and 2 were likewise tested for their statistical significances. It was found that for all cases, there was an overlap between the 1σ levels of the AMAX phase and DMIN phase parameters (not shown).

3. Discussion and Conclusions

This study reports, for the first time, that HILDCAA intervals are characterized by enhanced magnetospheric relativistic electrons. The intense substorm/convection events that comprise the high-intensity, long-duration, continuous *AE* intervals of the HILDCAAs are responsible for frequent and intense injections of anisotropic 10–100 keV electrons into the magnetosphere. These electrons are sources for the acceleration to

even higher MeV energies. Although most HILDCAAs are part of high-speed solar wind streams emanating from coronal holes [*Hajra et al.*, 2013], not all HSSs are HILDCAA events. Thus, the identification and use of HILDCAA events are more direct links to MeV electron acceleration. The enhancement of the fluxes is delayed by ~1.5 days from the onset of the HILDCAAs. The initial fluxes before and at $t = 0$ are lower for the events during the solar cycle ascending and solar maximum phases than for those during the solar cycle declining and solar minimum phases. The flux increases for the DMIN phase events are much larger (>50%) than for the AMAX phase events. Although the solar wind speed was slightly higher and lasted longer during the DMIN phases on average, the difference seems to be insignificant with respect to that of the large flux increases. Moreover, no other solar wind or magnetospheric parameter shows any major difference between the solar cycle phases. Thus, although the hypotheses that HILDCAAs lead to relativistic electron enhancements (more than just solar wind high-speed streams), a new feature is the much greater relativistic electron fluxes during the DMIN phases than during the AMAX phases.

What can be the explanation of this solar cycle phase dependence? One would expect that with higher solar wind speeds during the DMIN phases, this would lead to higher solar wind electric fields and polar cap potentials. However, this appears not to be the case from the data analyses portion of this statistical study. No such PCI or electric field relative enhancements were noted.

One important clue might be the lower flux base during the AMAX events. The average initial flux level before HILDCAA initiation for the AMAX events was ~800 $cm^{-2}\,s^{-1}\,sr^{-1}$, while the same for the DMIN events was >1000 $cm^{-2}\,s^{-1}\,sr^{-1}$. A possible factor controlling the initial/preevent flux level is the time between two consecutive events. If the time between geoeffective events is shorter, as will be the case during the declining phase of the solar cycle, when there are often two corotating HSSs per solar rotation, then the relativistic electron flux may not have sufficient time to return to the same quiet time level as the AMAX events. This may lead to higher preevent fluxes during the DMIN phases.

There are at least two possible reasons for the observed differences in relativistic electron acceleration between the DMIN and AMAX phases. Either the relativistic electron loss rates are higher during the rising and maximum phases or the acceleration process is more efficient during the declining and minimum phases. In either case, the answer probably lies with the chorus wave properties, since chorus is believed to be both a source of electron acceleration [*Horne and Thorne*, 1998; *Summers et al.*, 1998, 2004; *Roth et al.*, 1999; *Meredith et al.*, 2002, 2003; *Horne et al.*, 2003a, 2005] and losses [*Nakamura et al.*, 2000; *Lorentzen et al.*, 2001; *Thorne et al.*, 2005; *Tsurutani et al.*, 2013]. One thought is that with higher solar irradiance during solar maximum, the dayside magnetosphere will be populated with higher thermal plasma densities [*Jentsch*, 1976]. These higher plasma densities could act to reduce local wave phase speeds and enhance particle pitch angle scattering [*Tsurutani and Smith*, 1977], thus reducing the "seed" population of 10–100 keV electrons for relativistic electron growth. Another possibility is that with the higher thermal plasma densities during solar maximum, the ratio of the electron plasma frequency to the electron gyrofrequency ω_{pe}/Ω_e will also be higher. This will reduce the amount of acceleration, since the electron acceleration by whistler mode waves is more efficient for smaller ω_{pe}/Ω_e ratio [*Summers et al.*, 1998; *Horne et al.*, 2003b]. It is possible that both mechanisms are contributing to the greater relativistic electron acceleration during the DMIN phases.

Acknowledgments

The work of R.H. is financially supported by Fundação de Amparo à Pesquisa do Estado de São Paulo through postdoctoral research fellowship at INPE. One of the authors (E.E.) would like to thank the Brazilian CNPq (301233/2011-0) agency for the financial support. Portions of this research were performed at the Jet Propulsion Laboratory, California Institute of Technology under contract with NASA. We thank the two referees for their helpful comments/suggestions that have helped improve this paper.

The Editor thanks two anonymous reviewers for their assistance in evaluating this paper.

References

Alfvén, H. (1942), Existence of electromagnetic-hydrodynamic waves, *Nature*, *150*, 405–406.

Belcher, J. W., and L. Davis Jr. (1971), Large-amplitude Alfvén waves in the interplanetary medium: 2, *J. Geophys. Res.*, *76*, 3534–3563, doi:10.1029/JA076i016p03534.

DeForest, S. E., and C. E. McIlwain (1971), Plasma clouds in the magnetosphere, *J. Geophys. Res.*, *76*, 3587–3611, doi:10.1029/JA076i016p03587.

Guarnieri, F. L. (2006), The nature of auroras during high-intensity long-duration continuous AE activity (HILDCAA) events: 1998–2001, in *Recurrent Magnetic Storms: Corotating Solar Wind Streams*, *Geophys. Monogr. Ser.*, vol. 167, edited by B. T. Tsurutani et al., pp. 235–243, AGU, Washington, D. C.

Hajra, R., E. Echer, B. T. Tsurutani, and W. D. Gonzalez (2013), Solar cycle dependence of High-Intensity Long-Duration Continuous AE Activity (HILDCAA) events, relativistic electron predictors?, *J. Geophys. Res. Space Physics*, *118*, 5626–5638, doi:10.1002/jgra.50530.

Hajra, R., E. Echer, B. T. Tsurutani, and W. D. Gonzalez (2014), Solar wind-magnetosphere energy coupling efficiency and partitioning: HILDCAAs and preceding CIR-storms during solar cycle 23, *J. Geophys. Res. Space Physics*, *119*, doi:10.1002/2013JA019646.

Horne, R. B., and R. M. Thorne (1998), Potential waves for relativistic electron scattering and stochastic acceleration during magnetic storms, *Geophys. Res. Lett.*, *25*, 3011–3014, doi:10.1029/98GL01002.

Horne, R. B., and R. M. Thorne (2003), Relativistic electron acceleration and precipitation during resonant interactions with whistler-mode chorus, *Geophys. Res. Lett.*, *30*(10), 1527, doi:10.1029/2003GL016973.

Horne, R. B., N. P. Meredith, R. M. Thorne, D. Heynderickx, R. H. A. Iles, and R. R. Anderson (2003a), Evolution of energetic electron pitch angle distributions during storm time electron acceleration to megaelectronvolt energies, *J. Geophys. Res.*, *108*(A1), 1016, doi:10.1029/2001JA009165.

Horne, R. B., S. A. Glauert, and R. M. Thorne (2003b), Resonant diffusion of radiation belt electrons by whistler-mode chorus, *Geophys. Res. Lett.*, *30*(9), 1493, doi:10.1029/2003GL016963.

Horne, R. B., R. M. Thorne, S. A. Glauert, J. M. Albert, N. P. Meredith, and R. R. Anderson (2005), Timescale for radiation belt electron acceleration by whistler mode chorus waves, *J. Geophys. Res.*, *110*, A03225, doi:10.1029/2004JA010811.

Inan, U. S., T. F. Bell, and R. A. Helliwell (1978), Nonlinear pitch angle scattering of energetic electrons by coherent VLF waves in the magnetosphere, *J. Geophys. Res.*, *83*, 3235–3253.

Jentsch, V. (1976), Electron precipitation in morning sector of the auroral zone, *J. Geophys. Res.*, *81*, 135–146.

Kennel, C. F., and H. E. Petschek (1966), Limit on stable trapped particle fluxes, *J. Geophys. Res.*, *71*, 1–28, doi:10.1029/JZ071i001p00001.

Lorentzen, K. R., J. B. Blake, U. S. Inan, and J. Bortnik (2001), Observations of relativistic electron microbursts in association with VLF chorus, *J. Geophys. Res.*, *106*, 6017–6027, doi:10.1029/2000JA003018.

Meredith, N. P., R. B. Horne, R. H. A. Iles, R. M. Thorne, D. Heynderickx, and R. R. Anderson (2002), Outer zone relativistic electron acceleration associated with substorm-enhanced whistler mode chorus, *J. Geophys. Res.*, *107*(A7), 1144, doi:10.1029/2001JA900146.

Meredith, N. P., M. Cain, R. B. Horne, R. M. Thorne, D. Summers, and R. R. Anderson (2003), Evidence for chorus-driven electron acceleration to relativistic energies from a survey of geomagnetically disturbed periods, *J. Geophys. Res.*, *108*(A6), 1248, doi:10.1029/2002JA009764.

Nakamura, R., M. Isowa, Y. Kamide, D. N. Baker, J. B. Blake, and M. Looper (2000), SAMPEX observations of precipitating bursts in the outer radiation belt, *J. Geophys. Res.*, *105*, 15,875–15,885, doi:10.1029/2000JA900018.

Newell, P. T., T. Sotirelis, K. Liou, C. I. Meng, and F. J. Rich (2007), A nearly universal solar wind-magnetosphere coupling function inferred from 10 magnetospheric state variables, *J. Geophys. Res.*, *112*, A01206, doi:10.1029/2006JA012015.

Paulikas, G., and J. B. Blake (1979), Effects of the solar wind on magnetospheric dynamics: Energetic electrons at the synchronous orbit, in *Quantitative Modeling of Magnetospheric Processes*, *Geophys. Monogr. Ser.*, vol. 21, edited by W. Olsen, pp. 180–202, AGU, Washington, D. C.

Roth, I., M. A. Temerin, and M. K. Hudson (1999), Resonant enhancement of relativistic electron fluxes during geomagnetically active periods, *Ann. Geophys.*, *17*, 631–638.

Smith, E. J., and J. H. Wolfe (1976), Observations of interaction regions and corotating shocks between one and five AU: Pioneers 10 and 11, *Geophys. Res. Lett.*, *3*, 137–140, doi:10.1029/GL003i003p00137.

Summers, D., R. M. Thorne, and F. Xiao (1998), Relativistic theory of wave-particle resonant diffusion with application to electron acceleration in the magnetosphere, *J. Geophys. Res.*, *103*, 20,487–20,500, doi:10.1029/98JA01740.

Summers, D., C. Ma, N. P. Meredith, R. B. Horne, R. M. Thorne, and R. R. Anderson (2004), Modeling outer-zone relativistic electron response to whistler mode chorus activity during substorms, *J. Atmos. Sol. Terr. Phys.*, *66*, 133–146.

Summers, D., B. Ni, and N. P. Meredith (2007), Timescale for radiation belt electron acceleration and loss due to resonant wave-particle interactions: 2. Evaluation for VLF chorus, ELF hiss, and electromagnetic ion cyclotron waves, *J. Geophys. Res.*, *112*, A04207, doi:10.1029/2006JA011993.

Thorne, R. M., T. P. O'Brien, Y. Y. Shprits, D. Summers, and R. B. Horne (2005), Timescale for MeV electron microburst loss during geomagnetic storms, *J. Geophys. Res.*, *110*, A09202, doi:10.1029/2004JA010882.

Tsurutani, B. T., and W. D. Gonzalez (1987), The cause of high-intensity long-duration continuous AE activity (HILDCAAs): Interplanetary Alfvén wave trains, *Planet. Space Sci.*, *35*, 405–412.

Tsurutani, B. T., and E. J. Smith (1974), Postmidnight chorus: A substorm phenomenon, *J. Geophys. Res.*, *79*, 118–127, doi:10.1029/JA079i001p00118.

Tsurutani, B. T., and E. J. Smith (1977), Two types of magnetospheric ELF chorus and their substorm dependences, *J. Geophys. Res.*, *82*, 5112–5128, doi:10.1029/JA082i032p05112.

Tsurutani, B. T., C. M. Ho, E. J. Smith, M. Neugebauer, B. E. Goldstein, J. S. Mok, J. K. Arballo, A. Balogh, D. J. Southwood, and W. C. Feldman (1994), The relationship between interplanetary discontinuities and Alfvén waves: Ulysses observations, *Geophys. Res. Lett.*, *21*, 2267–2270, doi:10.1029/94GL02194.

Tsurutani, B. T., W. D. Gonzalez, A. L. C. Gonzalez, F. Tang, J. K. Arballo, and M. Okada (1995), Interplanetary origin of geomagnetic activity in the declining phase of the solar cycle, *J. Geophys. Res.*, *110*, 21,717–21,733.

Tsurutani, B. T., W. D. Gonzalez, F. L. Guarnieri, Y. Kamide, X. Zhou, and J. K. Arballo (2004), Are high-intensity long-duration continuous AE activity (HILDCAA) events substorm expansion events?, *J. Atmos. Sol. Terr. Phys.*, *66*, 167–176.

Tsurutani, B. T., O. P. Verkhoglyadova, G. S. Lakhina, and S. Yagitani (2009), Properties of dayside outer zone chorus during HILDCAA events: Loss of energetic electrons, *J. Geophys. Res.*, *114*, A03207, doi:10.1029/2008JA013353.

Tsurutani, B. T., R. B. Horne, J. S. Pickett, O. Santolik, D. Schriver, and O. P. Verkhoglyadova (2010), Introduction to the special section on Chorus: Chorus and its role in space weather, *J. Geophys. Res.*, *115*, A00F01, doi:10.1029/2010JA015870.

Tsurutani, B. T., E. Echer, F. L. Guarnieri, and W. D. Gonzalez (2011), The properties of two solar wind high speed streams and related geomagnetic activity during the declining phase of solar cycle 23, *J. Atmos. Sol. Terr. Phys.*, *73*, 164–177.

Tsurutani, B. T., G. S. Lakhina, and O. P. Verkhoglyadova (2013), Energetic electron ($>$ 10 keV) microburst precipitation, ~5-15 s X-ray pulsations, chorus, and wave-particle interactions: A review, *J. Geophys. Res. Space Physics*, *118*, 2296–2312, doi:10.1002/jgra.50264.